

ARTICLE

Open Access

Tree shrew as a new animal model to study the pathogenesis of avian influenza (H9N2) virus infection

Runfeng Li¹, Bing Yuan^{1,2}, Xueshan Xia³, Sheng Zhang¹, Qiuling Du¹, Chunguang Yang¹, Na Li¹, Jin Zhao¹, Yunhui Zhang², Rongping Zhang⁴, Yue Feng³, Jianlin Jiao⁵, Malik Peiris^{1,6}, Nanshan Zhong¹, Chris Ka Pun Mok^{1,6} and Zifeng Yang¹

Abstract

Outbreaks of avian influenza virus continue to pose threats to human health. Animal models such as the mouse, ferret, and macaque are used to understand the pathogenesis of avian influenza virus infection in humans. We previously reported that the tree shrew (*Tupaia belangeri*, family Tupaiidae), which is regarded as a “low-level primate”, has $\alpha 2,3$ - and $\alpha 2,6$ -linked sialic acid receptor distributions similar to those of humans and is potentially a useful mammalian model for studying mild human influenza (H1N1) virus infection. In this study, we used the tree shrew experimental model to investigate the pathogenesis of avian influenza A (H9N2) virus infection and the effect of the E627K mutation in the *PB2* gene, an adaptation to mammalian hosts. Evidence of disease, virus titers in the upper and lower respiratory tract, histopathology and induction of proinflammatory cytokines are described. We also established ex vivo culture models of tree shrew respiratory tissues to study the tropism and replication of the H9N2 virus. Our results demonstrated that the tree shrew is a viable new in vivo experimental model for avian influenza research that provides results comparable to those observed in ferrets. The disease spectrum and pathogenesis in tree shrews correlate well with what is observed in humans.

Introduction

Influenza A (H9N2) virus is the most widespread subtype of avian influenza found in poultry in Asia. In addition to the economic impact on the poultry industry, interspecies transmission of H9N2 viruses from poultry to humans has occurred repeatedly^{1–4}, and the virus poses a potential pandemic threat. Moreover, reassortment between H9N2 and other avian viruses has generated new

zoonotic subtypes, such as H5N1, H7N9, and H10N8, which have caused lethal zoonotic disease^{5–7}. The H9N2 viruses that are circulating in poultry in China have evolved into two major phylogenetic lineages: the H9N2/G1-like lineage, represented by A/Quail/Hong Kong/G1/97 (H9N2/G1), and the H9N2/Y280-like lineage, represented by A/Duck/Hong Kong/Y280/97 (H9N2/Y280)⁸. Although H9N2 virus can cause severe disease in immunocompromised patients, most human infections in immunocompetent persons are associated only with mild respiratory disease^{2–4}. In vivo studies have shown that a mutation from glutamic acid (E) to lysine (K) at amino acid residue 627 of the *PB2* gene is an important adaptation marker of avian influenza viruses that contributes to pathogenesis in mammalian hosts^{9–11}.

Mouse and ferret have been commonly used to study the pathogenesis of H9N2 viruses in mammalian hosts.

Correspondence: Zifeng Yang (jeffyah@163.com) or Chris Ka Pun Mok (ch02mcp@hku.hk)

¹State Key Laboratory of Respiratory Disease, National Clinical Research Center for Respiratory Disease, Guangzhou Institute of Respiratory Health, the First Affiliated Hospital of Guangzhou Medical University, Guangzhou, Guangdong, P.R. China

²Department of Respiration, First People's Hospital of Yunnan Province, Kunming, Yunnan, P.R. China

Full list of author information is available at the end of the article.

These authors contributed equally: Runfeng Li, Bing Yuan, Xueshan Xia.

© The Author(s) 2018



Open Access This article is licensed under a Creative Commons Attribution 4.0 International License, which permits use, sharing, adaptation, distribution and reproduction in any medium or format, as long as you give appropriate credit to the original author(s) and the source, provide a link to the Creative Commons license, and indicate if changes were made. The images or other third party material in this article are included in the article's Creative Commons license, unless indicated otherwise in a credit line to the material. If material is not included in the article's Creative Commons license and your intended use is not permitted by statutory regulation or exceeds the permitted use, you will need to obtain permission directly from the copyright holder. To view a copy of this license, visit <http://creativecommons.org/licenses/by/4.0/>.

However, the distribution of sialic acids (SA)—which act as receptors for influenza viruses—differs notably between mice and humans. Many influenza viruses that infect humans do not infect mice without prior adaptation. Meanwhile, H9N2 infection in mice causes severe inflammation in the lower part of the lung, which is not what is usually observed in humans^{12–14}. On the other hand, H9N2 viruses cause mild respiratory symptoms in the ferret, approximating human infection^{15,16}. However, the use of ferrets is limited by the relatively high cost and by the requirement for specially designed facilities and husbandry. *Cynomolgus* macaques have been used as experimental models for influenza^{17,18}. However, the SA receptor distribution in macaques does not parallel what is found in humans, and the facilities needed for macaques are not widely available.

The tree shrew (*Tupaia belangeri*, family Tupaiidae), indigenous to South Asia, Southeast Asia, and Southwest China, is classified as a separate taxonomic group of mammals that diverged from the primate order approximately 85 million years ago but still be considered as a “low-level primate” based on their close relationship¹⁹. Tree shrew is phylogenetically more closely related to humans than ferret and mice. We have previously shown that the tree shrew supports the replication of human influenza viruses without prior adaptation by serial passages and that the resulting infections bring mild disease symptoms resembling those in humans²⁰. Importantly, we showed that the distribution of SA receptors in the respiratory tract of tree shrews is similar to that of humans. Recently, the genome of the tree shrew has been fully sequenced, which will help to establish research tools for use in a tree shrew model²¹. In this study, we investigated whether the tree shrew is susceptible to infection with avian influenza (H9N2) virus, and we evaluated the virologic and immunological features of the H9N2-infected tree shrews through *in vivo* and *ex vivo* models.

Results

Infection with H9N2 viruses in tree shrews and ferrets showed comparable pathogenicity

To determine whether tree shrews are susceptible to infection with avian H9N2 virus without prior virus adaptation and to compare the pathogenicity with that in ferrets, we infected tree shrews and ferrets with 10^6 TCID₅₀ of the H9N2 Y280-wt virus. To investigate the role of the mammalian adaptation mutation PB2-E627K, a Y280 virus (PB2-E627K) by reverse genetics and tested in parallel with the Y280-wt virus (Fig. 1). With the exception of one tree shrew infected with Y280-wt virus, virus shedding was found in the nasal wash of all other tree shrews and ferrets 2 days after infection (Fig. 1a, d). The PB2-E627K mutant replicated more quickly than the wild-type isotype on day 2 in both tree shrews and ferrets. In

tree shrews, the virus could be detected until day 6 in the group challenged by the PB2-E627K mutant, while the wild-type virus was not found in any of the tree shrews on day 4. Shedding of both viruses was found until day 4 in the ferrets. Seroconversion to the challenged H9N2 subtype was found in all animals by hemagglutination inhibition (HI) assays, with antibody titers ranging from 80 to 640 in tree shrews and from 80 to 2560 in ferrets (Table 1). No animal died during the 14-day observation period.

We next compared changes in body temperature and body weight between tree shrews and ferrets following H9N2 virus infection. Although there was no statistically significant difference between the two groups, some tree shrews infected with the Y280-PB2-E627K viruses showed an increase in body temperature and an increased loss of body weight at 1-day postinfection compared to the mean value of those infected with the Y280-wt virus (Fig. 1b, c). Mock-infected tree shrews showed no significant change in body temperature, but their body weight increased (Supp Fig. 2a, b). In the ferret model, both the Y280-wt and Y280-PB2-E627K viruses brought an obvious increase in body temperature and weight loss during the first few days of infection. Ferret infected with the wild-type virus regained weight more quickly than those infected with the PB2-E627K mutant (Fig. 1e, f).

H9N2 virus replication in the nasal turbinates and lungs of tree shrews

We next investigated the replication of H9N2 viruses in different tissues of the respiratory tract in infected tree shrews. Nasal turbinate, throat, trachea, and lung tissues were collected at 2, 4, and 6 days postinfection (dpi), and the viral titer from the supernatant of the homogenized tissues was determined by TCID₅₀ assays. Consistent with the results from the nasal wash, Y280-PB2-E627K virus showed higher viral replication than Y280-wt in nasal turbinate at 2 dpi, but neither viruses showed any replication at 4 or 6 dpi (Fig. 2a). Replication in the throat and trachea could be found only in some tree shrews infected with either Y280-wt or Y280-PB2-E627K virus (Fig. 2b, c). Virus replication in the lungs was found only at 2 and 4 dpi in the two tree shrews infected with Y280-PB2-E627K virus (Fig. 2d).

Histopathology in the respiratory epithelium of tree shrews after infection with H9N2 virus

Inflammatory cells (lymphocytes and neutrophils) and focal edema on the submucosal layer of nasal turbinate were found in the tree shrews infected with Y280-wt virus at 2 dpi (Fig. 3a). The tissues isolated from the Y280-PB2-E627K-infected group showed an increased severity of lesions on the nasal turbinate, which were characterized by the identification of necrotic and sloughed epithelial

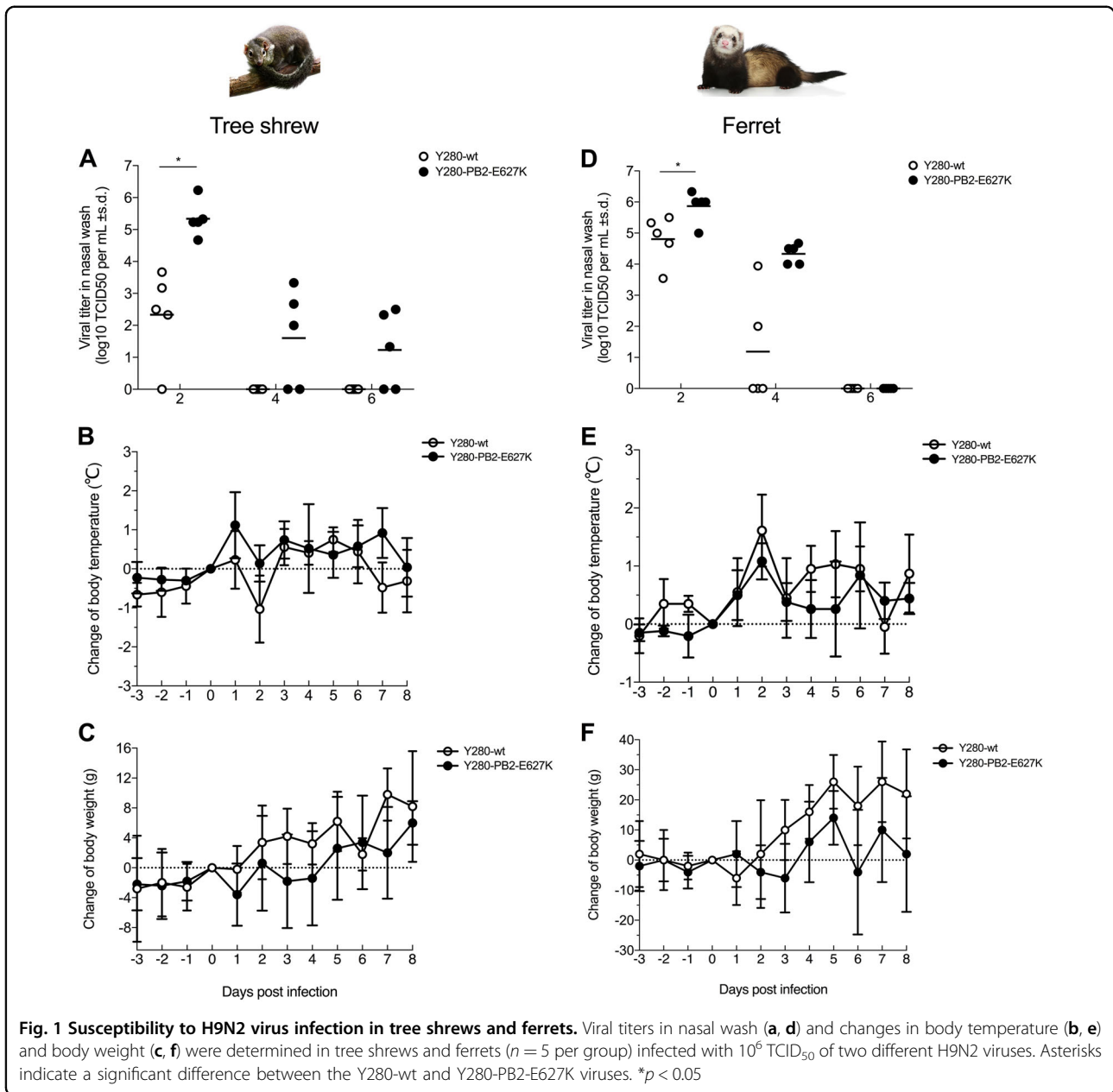


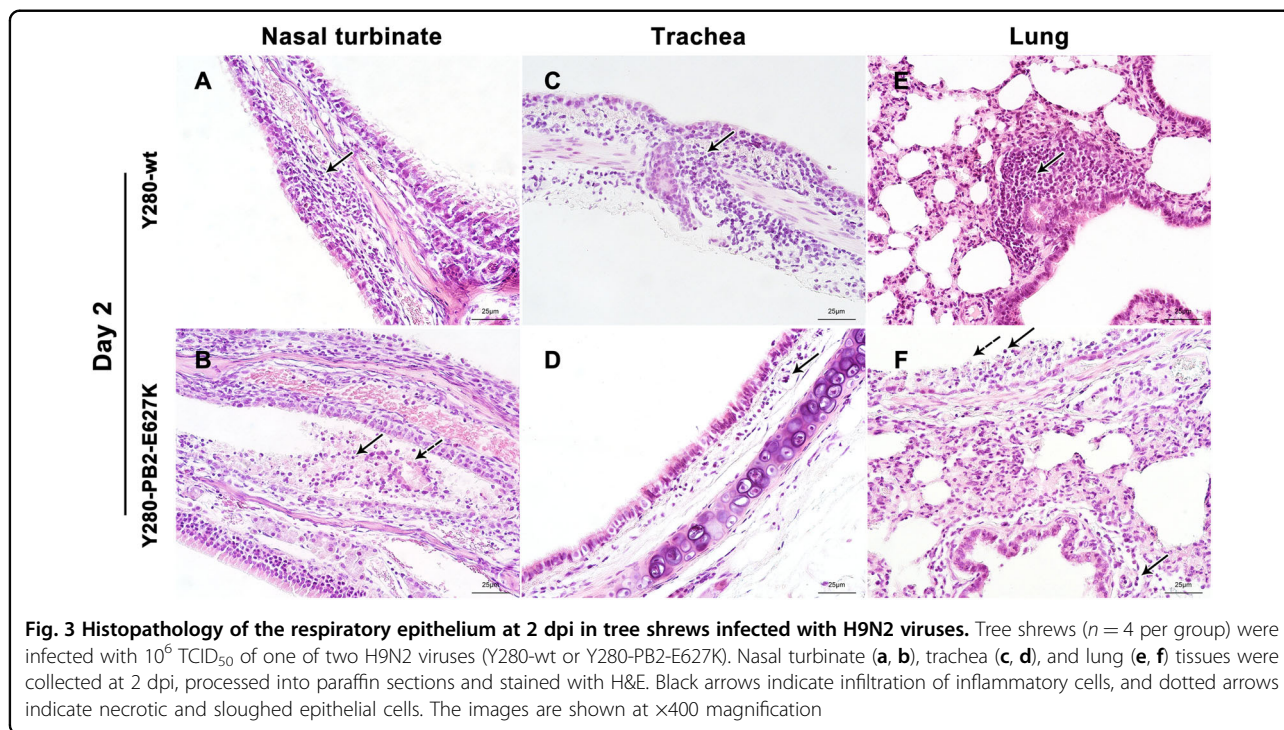
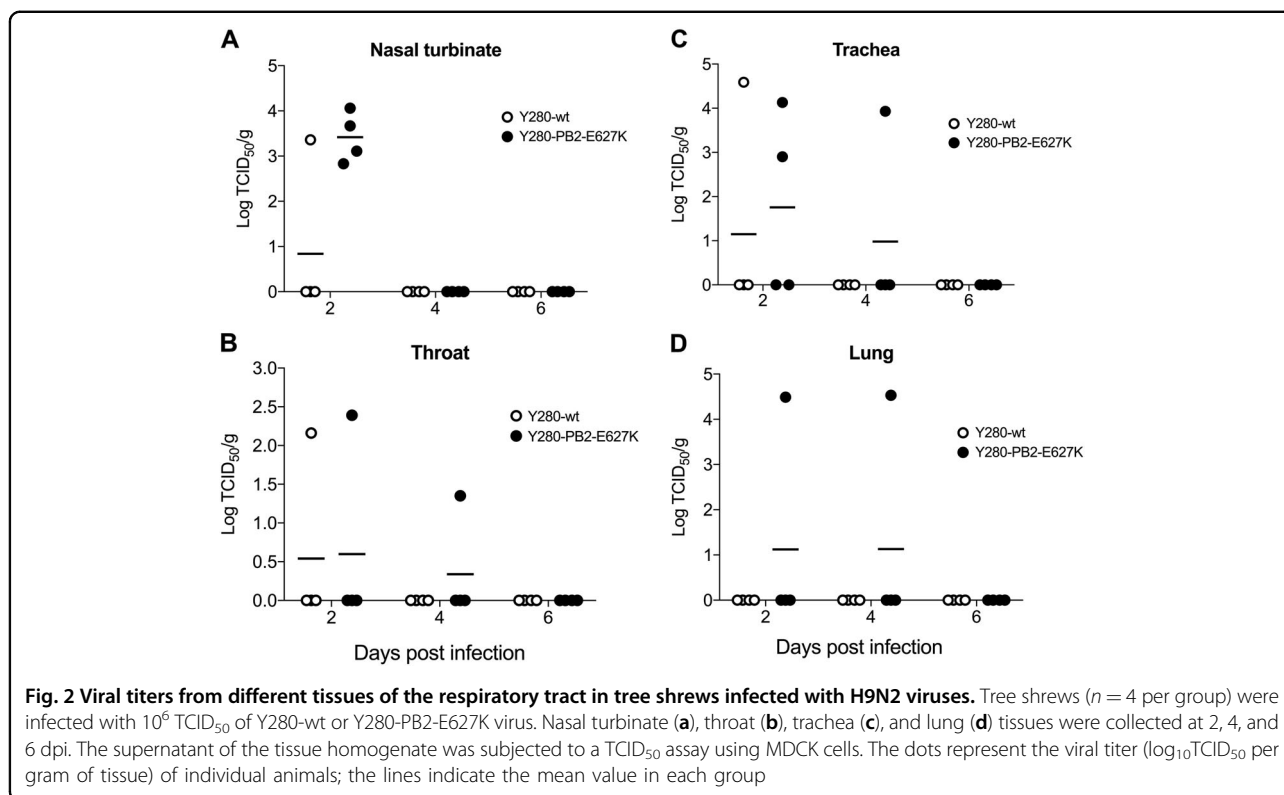
Table 1 Susceptibility of tree shrews and ferrets to infection with H9N2 viruses

Virus strain	Peak titer in nasal wash ± SD (day) ^a		(+) viral titer in nasal wash ^b		Seroconversion (range of the HI titer) ^c	
	Tree shrew	Ferret	Tree shrew	Ferret	Tree shrew	Ferret
Y280-wt	2.34 ± 1.41 (2)	4.81 ± 0.77(2)	4/5	5/5	5/5 (336, 80–640)	5/5(720, 80–1280)
Y280-PB2-E627K	5.34 ± 0.56 (2)	5.87 ± 0.50(2)	5/5	5/5	5/5 (512, 320–640)	5/5 (2030, 1280–2560)

^aPeak nasal wash titers are expressed as the mean log₁₀TCID₅₀/mL ± SD

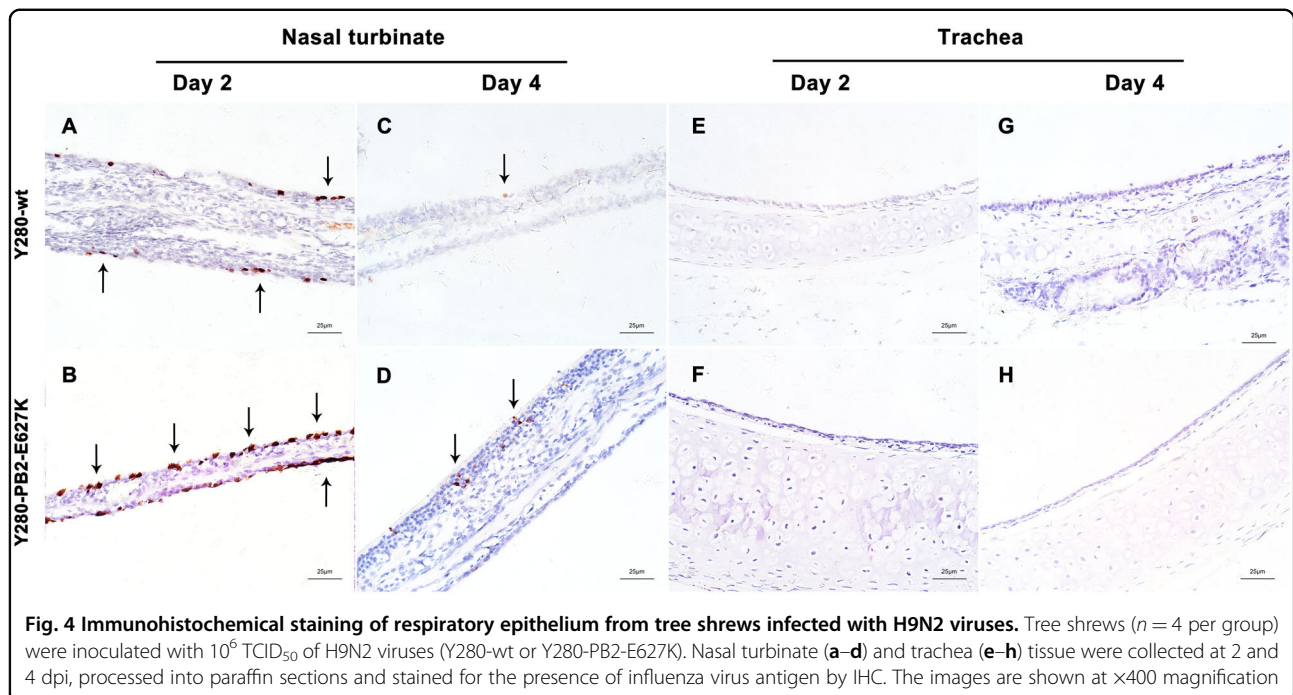
^bThe lower limit of detection was 10^{1.5} TCID₅₀/mL on day 2 postinfection

^cSerum samples were collected on day 21 postinfection, and the HI titers were determined by using chicken RBCs



cells, increased lymphocytic infiltration in the sub-mucosal/intramucosal layers and vascular dilatation (Fig. 3b). Increased expression of viral antigens was detected in the epithelium of nasal turbinate tissues from

the Y280-PB2-E627K-infected group compared to those infected with the Y280-wt virus (Fig. 4a–d). At 4 dpi, the severity of the lesions on the nasal turbinate was significantly improved in both groups (Supp Fig. 1a, b). The



tracheal epithelium of both groups showed mild lymphocytic inflammation of the submucosal/intramucosal layers (Fig. 3c, d and Supp Fig. 1C, D). No virus antigen was identified in the trachea obtained from either group (Fig. 4e–h). While there was no evidence of virus replication in the lung, the peribronchiolar epithelium of the Y280-wt-infected tree shrews still showed mild infiltration of macrophages and thickened alveolar walls at 2 and 4 dpi (Fig. 3e and Sup Fig. 1E). Virus replication was found in the lung tissues of two tree shrews infected with the Y280-PB2-E627K virus, one at 2 dpi and one at 4 dpi (Fig. 2d). Interestingly, the lung tissues isolated from the Y280-PB2-E627K-infected group, including those with and those without positive detection of virus replication, all showed increased severity of lesions, including apparent necrotic and sloughed cells as well as inclusion bodies in the mucosal layer of bronchiolar epithelium, compared to the tree shrews infected with the Y280-wt virus (Fig. 3f and Supp Fig. 4F). The histopathology and immunohistochemical staining of mock-infected tree shrews are shown as controls (Supp Fig. 2C, D).

Expression profile of cytokine mRNAs in tree shrews infected with the H9N2 viruses compared with mock-infected controls

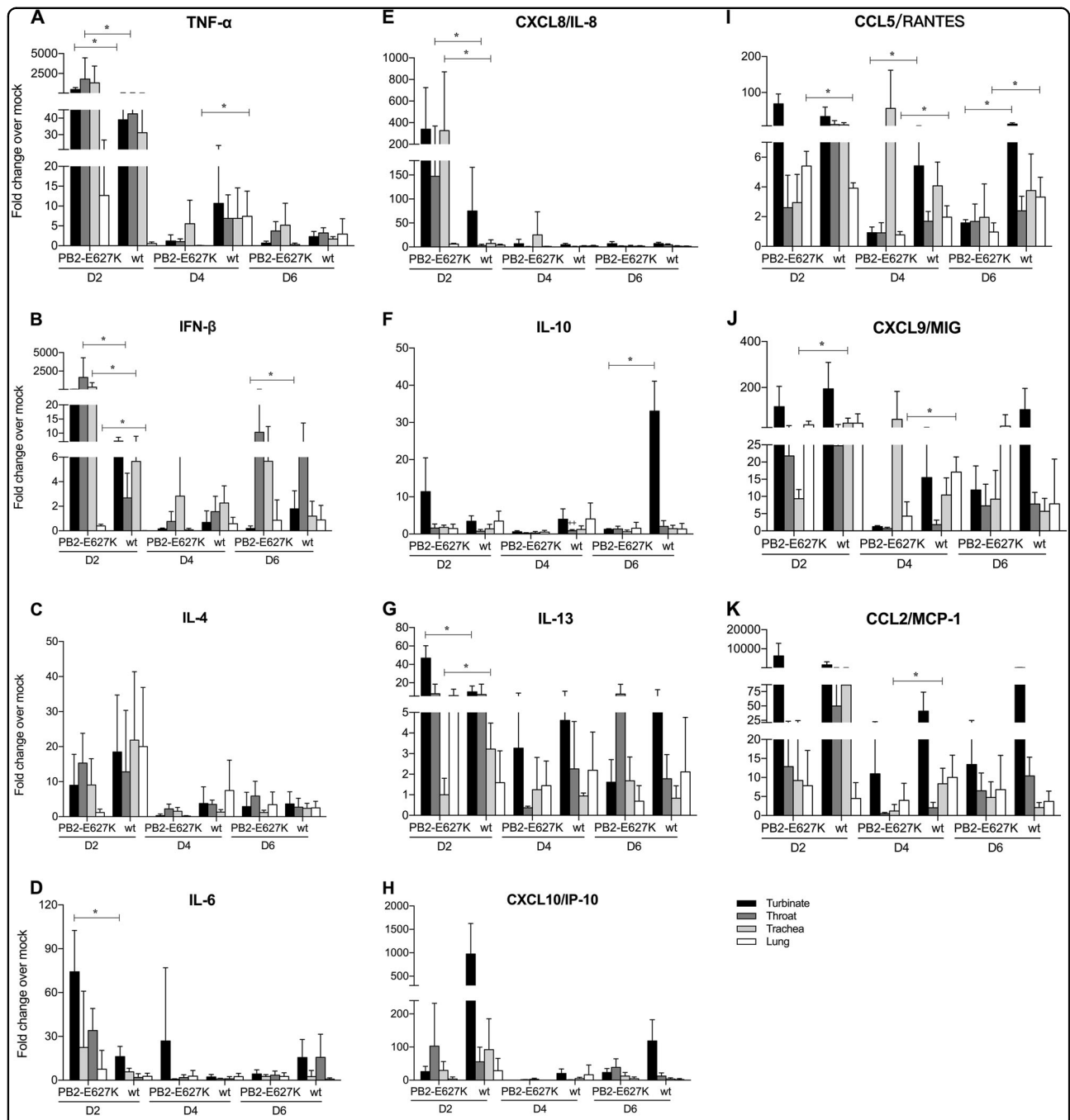
The mRNA expression profiles of selected cytokines, including *tumor necrosis factor α* (*TNF- α*), *interferon β* (*IFN- β*), *IL-4*, *IL-6*, *CXCL8* (*IL-8*), *IL-10*, *IL-13*, *CXCL10* (*IP-10*), *CCL5* (*RANTES*), *CXCL9* (*MIG*), and *CCL2* (*MCP-1*), were measured from nasal turbinate, throat, trachea, and lung tissues obtained from tree shrews

infected with the H9N2 viruses. The results are expressed as fold change compared to mock-infected tissue. In general, tree shrews infected with either wild-type or PB2 mutant H9N2 virus showed higher induction of cytokines in the examined tissues than the uninfected controls. In general, the expression of all cytokines peaked at 2 dpi (Fig. 5). At this time point, we found that the mRNA levels of *TNF- α* , *IFN- β* , *IL-8*, *IL-13*, and *IL-6* in the upper respiratory tract (nasal turbinate or throat) and *IL-8*, *RANTES*, and *IFN- β* in the lower respiratory tract (trachea or lung) were significantly higher in the tree shrews infected with Y280-PB2-E627K than in those infected with Y280-wt virus. On the other hand, Y280-wt virus triggered significantly higher mRNA expression of *MIG* (2 dpi, trachea; 4 dpi, lung), *IL-13* (2 dpi, trachea), *MCP-1* (4 dpi, trachea), and *IL-10* (6 dpi, nasal turbinate) than Y280-PB2-E627K virus.

Virus replication and cytokine mRNA expression of the tree shrew ex vivo cultures after H9N2 virus infection

We established an ex vivo culture model (nasal turbinate, trachea and lung) to compare the replication of the H9N2 virus and its PB2-E627K mutant. Under comparable infection conditions, we found that the Y280-PB2-E627K virus replicated more efficiently in the nasal turbinate, trachea, and lung tissues than the Y280-wt virus did ($p < 0.05$) (Fig. 6a–c).

The mRNA expression profiles of the selected cytokines were also measured from the ex vivo cultures after infection with H9N2 viruses (Fig. 7). The cytokine levels of *TNF- α* (24 h and 48 h), *IFN- β* (24 h), *IL-8* (48 h), *IL-10*

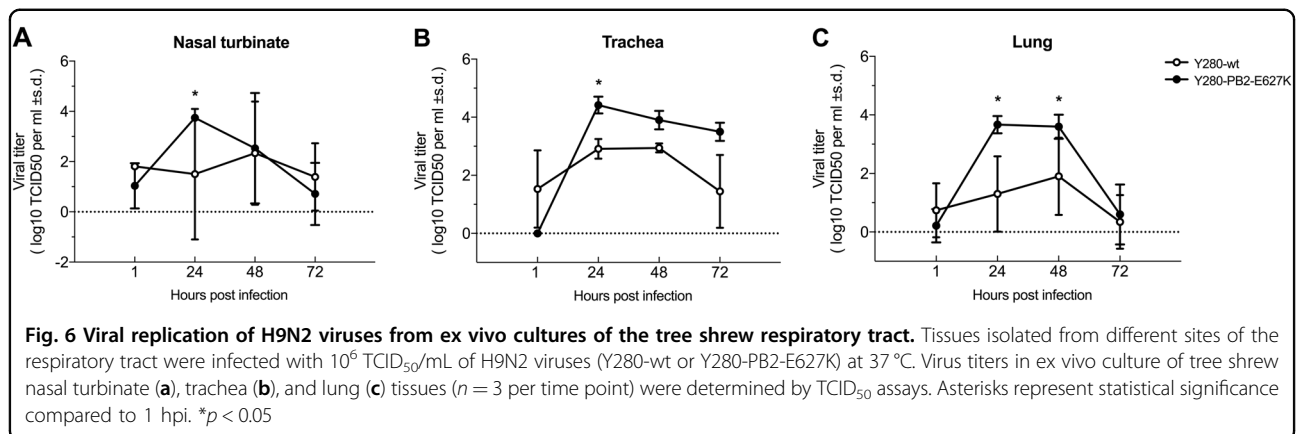


(72 h), *IL-4* (24 h), and *IL-13* (72 h) were significantly higher in the ex vivo lung tissues infected with the Y280-PB2-E627K virus than in those infected with Y280-wt virus. In contrast, higher levels of *IL-8* (24 h), *RANTES* (24 h), *IP-10* (24 h), and *IL-10* (48 h) in the tracheas as well as *IL-6* (24 h) and *IP-10* (72 h) in the lungs were found in

the Y280-w-infected group than in the Y280-PB2-E627K-infected group.

Discussion

Our study aimed to characterize the susceptibility of tree shrews to avian H9N2 virus infection as part of an

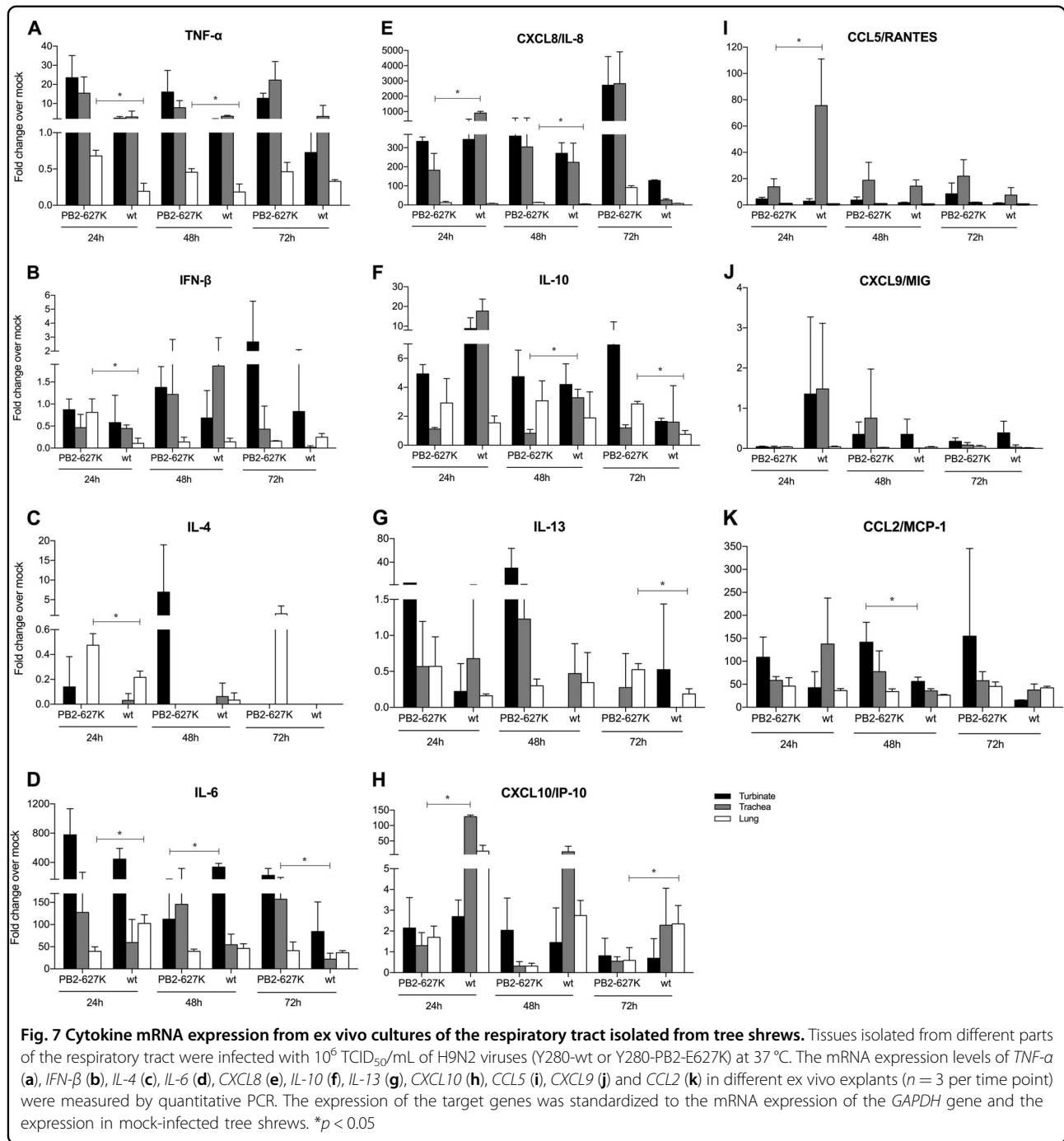


investigation to determine whether this experimental animal model is useful for studying the pathogenesis of avian influenza viruses in mammals. Unlike those with H5N1 or H7N9 viruses, patients with H9N2 infection mainly manifest mild upper respiratory symptoms, including fever, coryza, sore throat, and inflamed oropharynx, analogous to the effects of seasonal influenza viruses^{2,22,23}. We found that infection with the wild-type avian H9N2 virus (Y280-wt) showed transient virus shedding without an obvious increase in body temperature or weight loss. However, our histological findings clearly identified evidence of infection, with inflammatory cells and focal edema observed in the submucosal layer of the nasal turbinates at the early stage of infection. Although one tree shrew showed no virus shedding after infection with the H9N2 wild-type virus, the high antibody titer against the H9N2/Y280 strain in the blood of this tree shrew suggested that there was asymptomatic infection.

Mutations in the *PB2* gene contribute to the pathogenicity of avian influenza virus in mammalian hosts^{9–11}. Specifically, the PB2-E627K mutation is associated with an increase in the virulence and replication of the avian influenza virus in both in vitro and in vivo models. We also found that H9N2 virus with the E627K mutation (Y280-PB2-E627K) was shed by tree shrews in higher quantities and for a longer period than its wild-type control. The virus was disseminated more widely in the respiratory tract, and there was evidence of inflammation in the lower lung in some but not all tree shrews. Taken together, our results showed that the tree shrew is highly susceptible to avian influenza H9N2 virus infection.

Different experimental animal models have been used to simulate the outcomes of avian influenza virus infection in humans. Mice and ferrets are the two commonly used experimental animal models used for the in vivo study of avian influenza virus. Macaques have occasionally been used as an experimental model but are extremely

costly; additionally, there are ethical issues with their use, and the outcomes of infection in macaques do not closely mimic those observed in humans. We and others have previously studied the pathogenesis of H9N2 virus infection and the contribution of the PB2-E627K mutation in mice^{12–14}. It was consistently found that H9N2 virus with this mammalian adaptation mutation usually caused more severe disease and greater lethality and weight loss in mice than in humans. This more pronounced phenotype in mice may be due to the availability of α 2,3-linked SA receptors in the upper respiratory tract of mice, which would facilitate lower lung infection even by intranasal inoculation of the virus²⁴. The human and ferret respiratory tract predominantly has α 2,6-linked SA receptors in the upper respiratory tract, with α 2,3-linked SA receptors being present only in the lower respiratory tract. In our study, both ferrets and tree shrews supported the replication of the H9N2 virus, and this replication was further enhanced by the PB2-E627K mutation. However, the overall severity of infection in these two animal models remained mild, which is comparable to what is observed in humans. The ferret has been used as a model to assess the pathogenicity and transmissibility of the H9N2 virus because it has a distribution of α 2,3 and α 2,6 SA receptors that resembles the distribution seen in the human respiratory tract²⁵. In our experiments, the wild-type H9N2/Y280 virus replicated efficiently in ferrets even without the PB2-E627K mutation, while the difference between the wild type and the PB2 mutant was more significant in tree shrews, supporting the previous finding that tree shrews are susceptible to avian H9N2 virus infection. Moreover, our newly established tree shrew ex vivo cultures demonstrated that the PB2-E627K mutation enhanced the early cycles of H9N2 virus replication in the nasal turbinate and trachea, in which the kinetics were consistent with our findings from in vivo infection. Interestingly, the PB2-E627K mutant clearly replicated more efficiently than the wild-type virus in the



ex vivo study, while virus replication was observed only in the lungs of two tree shrews that were infected with the mutant. This result suggests that the PB2-E627K mutant has adapted by gaining the ability to replicate in the lower lung, but replication in this site may not occur in every infected individual and may be caused by other factors, which is similar to the situation in humans.

The induction of proinflammatory cytokine and chemokine expression has been shown to contribute to the

pathogenesis of avian influenza virus infection²⁶. We established a set of primers that can detect the mRNA level of 11 cytokines in the tree shrew. Elevated levels of cytokines were detected in the tissues isolated from the respiratory tract after infection with either the wild type or the PB2 mutant compared to the levels in the uninfected control, suggesting that infection with H9N2 virus can trigger innate immune responses in tree shrews. We found that the increase in proinflammatory cytokines in

the *in vivo* experiments generally peaked at day 2 and decreased at day 4, matching the viral titers detected in nasal wash at the corresponding time point, which indicates a strong correlation between cytokine expression and virus replication in the upper respiratory tract. Transient cytokine expression during early infection was also reported in ferrets^{27,28}. However, we did not find similar cytokine profiles between the *in vivo* and *ex vivo* experiments. This result is understandable, as the results from these two experiments were based on different infection conditions. While the former showed the regulation of cytokines in tree shrews under pathological conditions, the latter reflected the cytokine expression phenotype of wild-type H9N2 and its PB2 mutant in different tissues. Thus, the results from the two experimental settings provide different angles from which to characterize the pathogenesis of the virus.

In conclusion, our study further demonstrates the potential of the tree shrew as an additional experimental animal model for investigating the pathogenesis of influenza. The virus replication patterns and phenotype mimic what is observed with humans and ferrets. As an experimental model, the tree shrew is smaller in size, easier to handle, less aggressive and less expensive in terms of the cost per animal than ferrets (approximately 1/10 of the price). Importantly, tree shrews are evolutionarily closer to humans and primates than ferrets are^{19,21}.

Materials and methods

Viruses and cells

H9N2 virus A/duck/Hong Kong/Y280/97 (Y280-wt) and its PB2-E627K mutant (Y280-PB2-E627K) were grown in 9- to 11-day-old specific-pathogen-free (SPF) chicken eggs. MDCK cells were maintained in Dulbecco's modified Eagle's medium supplemented with 10% fetal bovine serum at 37 °C with 5% CO₂.

In vivo experiments

Tree shrews (female/male, 100~130 g) and ferrets (female, 900~1000 g) were purchased from the Faculty of Life Science and Technology, Kunming University of Science and Technology, Kunming, China. The animals were confirmed as serologically negative for the H9N2 Y280-wt virus before use. The animals were first anesthetized via intraperitoneal injection of 3% pentobarbital sodium dissolved in PBS and inoculated intranasally with Y280-wt or Y280-PB2-E627K virus (day 0). Body temperature and body weight were recorded daily using subcutaneous transponders (IPTT-300; Bio Medic Data Systems Inc., Seaford, Delaware), starting 4 days prior to infection. At days 2, 4, and 6 postinfection, 0.25 mL (0.125 mL per nostril) of PBS was instilled into the nostrils of the infected animals and allowed to exit into a Petri

dish. The fluid (nasal wash) was collected for virus titration using the TCID₅₀ assay in MDCK cells. Seroconversion of the animals was tested by HI assays. All animals used in the experiments were humanely euthanized at day 21 postinfection. At days 2, 4, and 6 postinfection, four tree shrews were randomly selected for euthanasia, and nasal turbinate, throat, trachea, and lung tissues were obtained. The left and right nasal turbinates and lungs, as well as the left and right sides of the trachea, were set aside in equal portions. One portion was used for histopathological analysis and immunostaining with anti-influenza NP antibody. Another portion was homogenized with PBS supplemented with ofloxacin, amphotericin B, penicillin, and streptomycin followed by centrifugation at 13,000 × g, 4°C. The virus titer in the supernatant was determined by a TCID₅₀ assay, and total RNA from the cell debris was extracted to measure the mRNA levels of the selected cytokines and chemokines.

Ex vivo experiments

Ex vivo cultures of nasal turbinate, trachea, and lung tissue were carried out as previously described²⁹. Briefly, the tissue blocks were first infected with 1 mL of 10⁶ TCID₅₀ influenza viruses and washed with warm PBS five times after 2 h of incubation. The tissue blocks were then cultured with fresh medium (F-12K supplemented with L-glutamine, ofloxacin, amphotericin B, 100 U/mL penicillin, 100 µg/mL streptomycin, and 1.5 µg/mL TPCK) at 37 °C. At 1, 24, 48, and 72 hpi, the supernatant was collected for TCID₅₀ assays. The tissue blocks were collected and homogenized with TRIzol (Invitrogen, USA). Total RNA was then extracted, after which the mRNA expression of the cytokines was measured using quantitative PCR.

Quantification of mRNA

Total RNA was converted to cDNA using Prime-Script™ RT Master Mix (Takara), and quantitative PCR was then performed with 2× H-TECH SYBR qPCR Mix according to the manufacturer's protocols. The levels of cytokine mRNA expression were reported as fold changes compared to the results from mock-infected tree shrews. The primers were designed using Primer 5.0 and are listed in Supplementary Table 1.

Histology and immunohistochemistry

The tissues isolated from the respiratory tract were first fixed with 10% neutral buffered formalin, embedded in paraffin, sectioned at 3 µm and stained with hematoxylin and eosin (H&E) as previously described³⁰. Immunohistochemical staining of the influenza nucleoprotein in the tissues was performed as follows. Four-micron-thick sections were treated with 0.1% Pronase (Roche

10165921001, Mannheim, Germany) in Tris buffer (1 M, pH 7.2) at 37 °C for 15 min, transferred to 95 °C for 15 min, and then blocked with 3% H₂O₂ for 20 min, followed by treatment with a Streptavidin/Biotin Blocking Kit (Cat. No. SP-2002, Vector Labs, Burlingame, CA). After being blocked with 10% normal goat serum for 20 min, the sections were incubated with 1/10 HB65 (EVL anti-influenza NP, subtype A) primary antibody for 1 h at room temperature, followed by incubation with biotinylated goat anti-mouse secondary antibody (Cat. No. ab64257; Abcam, Cambridge, MA, USA) for 30 min at 37 °C. After incubation with the Vectastain ABC Kit (Cat. No. PK-6100, Vector Lab, Burlingame, CA), the sections were developed with the Vector NovaRED™ Substrate Kit (Cat. No. SK-4800, Vector Lab, Burlingame, CA).

Statistics

Statistical analysis was performed using GraphPad Prism 7.0 software. Differences in viral titers and mRNA expression among groups were compared using an unpaired, parametric *t* test or the Mann–Whitney *U* test. *P* values < 0.05 were considered significant.

Data availability

The datasets generated and/or analyzed during the current study are available from the corresponding author upon request.

Acknowledgements

This work was supported by the National Natural Science Foundation of China (81471937); by the Yangcheng Scholars Research Fund for Guangzhou Municipal Universities (1201561571); by the Science and Technology Program of Guangzhou Municipal Universities (1201410111); by the Science and Technology Program of Guangzhou (201504010032); and by the Research Grants Council of the Hong Kong Special Administrative Region, China, through the Theme-Based Research Scheme (Ref: T11-705/14N).

Author details

¹State Key Laboratory of Respiratory Disease, National Clinical Research Center for Respiratory Disease, Guangzhou Institute of Respiratory Health, the First Affiliated Hospital of Guangzhou Medical University, Guangzhou, Guangdong, P.R. China. ²Department of Respiration, First People's Hospital of Yunnan Province, Kunming, Yunnan, P.R. China. ³Faculty of Life Science and Technology, Kunming University of Science and Technology, Kunming, P.R. China. ⁴School of Pharmaceutical Science & Yunnan Key Laboratory of Pharmacology for Natural Products, Kunming Medical University, Kunming, Yunnan, P.R. China. ⁵Technology Transfer Center, Kunming Medical University, Kunming, Yunnan, P.R. China. ⁶The HKU–Pasteur Research Pole, School of Public Health, Li Ka Shing Faculty of Medicine, The University of Hong Kong, Hong Kong, China

Authors' contributions

R.L., M.P., N.Z., C.K.P.M., and Z.Y. designed the study, analyzed and interpreted the data, and wrote the manuscript. R.L., B.Y., X.X., S.Z., Q.D., C.Y., N.L., J.Z., Y.Z., R.Z., Y.F., and J.J. performed the experiments.

Conflict of interest

The authors declare that they have no conflict of interest.

Publisher's note

Springer Nature remains neutral with regard to jurisdictional claims in published maps and institutional affiliations.

Supplementary Information accompanies this paper at (<https://doi.org/10.1038/s41426-018-0167-1>).

Received: 10 July 2018 Revised: 30 August 2018 Accepted: 2 September 2018

Published online: 10 October 2018

References

- Sullivan, K. M., Monto, A. S. & Longini, I. M. Jr. Estimates of the US health impact of influenza. *Am. J. Public Health* **83**, 1712–1716 (1993).
- Peiris, M. et al. Human infection with influenza H9N2. *Lancet* **354**, 916–917 (1999).
- Butt, K. M. et al. Human infection with an avian H9N2 influenza A virus in Hong Kong in 2003. *J. Clin. Microbiol.* **43**, 5760–5767 (2005).
- Pan, Y. et al. Human infection with H9N2 avian influenza in northern China. *Clin. Microbiol. Infect.* **24**, 321–323 (2018).
- Gao, H. N. et al. Clinical findings in 111 cases of influenza A (H7N9) virus infection. *N. Engl. J. Med.* **368**, 2277–2285 (2013).
- Guan, Y., Shortridge, K. F., Krauss, S. & Webster, R. G. Molecular characterization of H9N2 influenza viruses: were they the donors of the “internal” genes of H5N1 viruses in Hong Kong? *Proc. Natl. Acad. Sci. USA* **96**, 9363–9367 (1999).
- Qi, W. et al. Genesis of the novel human-infecting influenza A(H10N8) virus and potential genetic diversity of the virus in poultry, China. *Eur. Surveill.* **19**, pii: 20841 (2014).
- Li, C. et al. Evolution of H9N2 influenza viruses from domestic poultry in Mainland China. *Virology* **340**, 70–83 (2005).
- Sang, X. et al. Rapid emergence of a PB2-E627K substitution confers a virulent phenotype to an H9N2 avian influenza virus during adoption in mice. *Arch. Virol.* **160**, 1267–1277 (2015).
- Mänz, B., Schwemmler, M. & Brunotte, L. Adaptation of avian influenza A virus polymerase in mammals to overcome the host species barrier. *J. Virol.* **87**, 7200–7209 (2013).
- Zambon, M. C. The pathogenesis of influenza in humans. *Rev. Med. Virol.* **11**, 227–241 (2001).
- Wang, C., Lee, H. H., Yang, Z. F., Mok, C. K. & Zhang, Z. PB2-Q591K mutation determines the pathogenicity of avian H9N2 influenza viruses for mammalian species. *PLoS ONE* **11**, e0162163 (2016).
- Tian, J. et al. A single E627K mutation in the PB2 protein of H9N2 avian influenza virus increases virulence by inducing higher glucocorticoids (GCs) level. *PLoS ONE* **7**, e38233 (2012).
- Wu, R. et al. Multiple amino acid substitutions are involved in the adaptation of H9N2 avian influenza virus to mice. *Vet. Microbiol.* **138**, 85–91 (2009).
- Wan, H. et al. Replication and transmission of H9N2 influenza viruses in ferrets: evaluation of pandemic potential. *PLoS ONE* **3**, e2923 (2008).
- Li, X. et al. Genetics, receptor binding property, and transmissibility in mammals of naturally isolated H9N2 Avian Influenza viruses. *PLoS Pathog.* **10**, e1004508 (2014).
- Rimmelzwaan, G. F. et al. Pathogenesis of Influenza A (H5N1) virus infection in a primate model. *J. Virol.* **75**, 6687–6691 (2001).
- Siegers, J. Y. et al. Novel avian-origin influenza A (H7N9) virus attachment to the respiratory tract of five animal models. *J. Virol.* **88**, 4595–4599 (2014).
- Xiao, J., Liu, R. & Chen, C. S. Tree shrew (*Tupaia belangeri*) as a novel laboratory disease animal model. *Zool. Res.* **38**, 127–137 (2017).
- Yang, Z. F. et al. The tree shrew provides a useful alternative model for the study of influenza H1N1 virus. *Virology* **45**, 111 (2013).
- Fan, Y. H. et al. Genome of the Chinese tree shrew. *Nat. Commun.* **4**, 1426 (2013).
- Guo, Y., Li, J. & Cheng, X. Discovery of men infected by avian influenza A (H9N2) virus. *Zhonghua Shi Yan He Lin. Chuang Bing. Du Xue Za Zhi* **13**, 105–108 (1999).
- Saito, T. et al. Characterization of a human H9N2 influenza virus isolated in Hong Kong. *Vaccine* **20**, 125–133 (2001).
- Ibricevic, A. et al. Influenza virus receptor specificity and cell tropism in mouse and human airway epithelial cells. *J. Virol.* **80**, 7469–7480 (2006).
- Belsler, J. A., Katz, J. M. & Tumpey, T. M. The ferret as a model organism to study influenza A virus infection. *Dis. Models Mech.* **4**, 575–579 (2011).
- La Gruta, N. L., Kedzierska, K., Stambas, J. & Doherty, P. C. A question of self-preservation: immunopathology in influenza virus infection. *Immunol. Cell Biol.* **85**, 85–92 (2007).

27. Belser, J. A., Maines, T. R., Gustin, K. M., Katz, J. M. & Tumpey, T. M. Kinetics of viral replication and induction of host responses in ferrets differs between ocular and intranasal routes of inoculation. *Virology* **438**, 56–60 (2013).
28. Carolan, L. A. et al. Characterization of the localized immune response in the respiratory tract of ferrets following infection with influenza A and B viruses. *J. Virol.* **90**, 2838–2848 (2015).
29. Chan, R. W. et al. Tissue tropism of swine influenza viruses and reassortants in ex vivo cultures of the human respiratory tract and conjunctiva. *J. Virol.* **85**, 11581–11587 (2011).
30. van den Brand, J. M. et al. Comparison of temporal and spatial dynamics of seasonal H3N2, pandemic H1N1 and highly pathogenic avian influenza H5N1 virus infections in ferrets. *PLoS ONE* **7**, e42343 (2012).